

Accurate Extrinsic Prediction of Physical Systems Using Transformers

Arnaud Pannatier*

Kyle Matoba†

François Fleuret‡

Abstract

Accurate high-altitude wind forecasting is important for air traffic control. And the large volume of data available for this task makes deep neural network-based models a possibility. However, special methods are required because the data is measured only sparsely: along the main aircraft trajectories and arranged sparsely in space, namely along the main air corridors. Several deep learning approaches have been proposed, and in this work, we show that Transformers can fit this data efficiently and are able to extrapolate coherently from a context set.

We show this by an extensive comparison of Transformers to numerous existing deep learning-based baselines in the literature. Besides high-altitude wind forecasting, we compare competing models on other dynamical physical systems, namely those modelled by partial differential equations, in particular the Poisson equation and Darcy Flow equation. For these experiments, in the case where the data is arranged non-regularly in space, Transformers outperform all the other evaluated methods. We also compared them in a more standard setup where the data is arranged on a grid and show that the Transformers are competitive with state-of-the-art methods, even though it does not require regular spacing. The code and datasets of the different experiments will be made publicly available at publication time.

Keywords: Transformers, Air Traffic Control, Deep Learning, Dynamical Systems

1 Introduction

Air Traffic Controllers (ATCs) require reliable wind speed forecasts to organize the airspace safely, but relying on traditional weather forecasts is not sufficient in the altitude at which they operate, because large-scale dynamical solvers have an insufficient resolution their. At cruising altitudes, one cannot rely on precise and fixed weather stations and one has to default to using airplanes' measurements which are available only sparsely in space, along the main air corridors. But ATCs only need these reliable forecasts over their decision window, which is in the order of 30 minutes. Over that horizon, called nowcasting, one gets the most accurate forecast by extrapolating from the latest measures available rather than trying to solve expensive numerical equations solvers. Deep learning methods are a good match for that problem as they can exploit efficiently the high availability of the data.

Still one has to find a way of encoding this sparsely recorded data as it comes as a set of points spread along routes over airspace. Transformers [17], can be made to handle inputs in a permutation-invariant way, which is necessary for predicting from point sets. Given the success that Transformers have had in other application areas of deep learning, it thus makes sense to ask whether wind prediction for ATC, and the prediction of physical systems more generally, can benefit from using Transformers. Another option would be to model the space using a mesh as the underlying structure has the advantage that they are well-suited to modelling pairwise interactions, this approach is used in Graph Element Networks (GEN) [1] for example.

This work shows that Transformers are better suited than GENs for nowcasting wind speed at high altitudes. We found, in particular, using a Transformer for wind nowcasting leads to an increase in forecast accuracy over existing methods and other deep learning methods. We conducted a comparative study on different synthetic task modelling partial differential equations (PDEs). We used the Poisson equation dataset developed in [1] and adapted the Darcy Flow equation dataset of [10] to compare the models on tasks of various complexity. We concluded that Transformers with the same number of parameters outperform GEN on wind nowcasting and Darcy Flow simulation, on the Poisson equation, we found that Transformers are obtaining similar results while being less affected by change in the scale of parameters.

The contributions of this work are the following:

- Improved performance on our earlier work ([12]) on an important practical problem.
- Developing a method to apply Transformers to extrinsic forecasting of spatial processes.
- Establishing the strong performance of Transformers on several other important problems in the physical sciences through a unified evaluation framework.
- Uncovering some implementation problems in competing models.

*Idiap Research Institute and EPFL, arnaud.pannatier@idiap.ch

†Idiap Research Institute and EPFL, kyle.matoba@epfl.ch

‡Université de Genève, francois.fleuret@unige.ch

The code and datasets of the different experiments will be made available at publication time.

2 Related Work

This work builds upon [12] and uses the same dataset. [12] introduces a smart Gaussian Kernel Averaging (GKA) model, that forms a weighted average of the context measurement to output a prediction where weights are a function of the distance to the target point and the absolute position in the space via a multi-layer perceptron (MLP). The main flaw of this method is that the range of the value that it can use for forecasting is a convex combination of the one that it has in its context, which limits its extrapolating capabilities. This means that if the wind magnitude is linearly increasing over a few hours, the model cannot spot this trend and forecasts contain therefore a lag. Transformers address this flaw as they can combine and transform each value of the context to create a prediction. Another methodological limitation of GKA is that it needs to have context values that live in the same space than the output values. This makes it impossible to use this model as a deep-learning-based PDEs solver since often one wants to predict the value of a given variable. For example, in Figure 5 we show an example where we wish to model the mapping from a thermal coefficient to the solution of a PDE – here the inputs and outputs live in completely different spaces.

The Finite Element Method (FEM) approach [5] uses a non-regular graph that can be denser in the more complex regions and coarser in the more regular regions. GEN [1] adapts the FEM logic to deep learning models and aims to model dynamical systems using a non-regular graph with nodes that live in an underlying space \mathbb{X} . Each measurement (x, i) is encoded using a small MLP into latent vectors that are then interpolated into the values of the nodes of the graphs. The model then processes this latent variable using $T \in \mathbb{N}$ steps of message passing. To predict a value at a new query position, the model linearly extrapolates in latent space and decodes using a small MLP modelling the transformation from latent to output space.

Other graph-based approaches exist for modelling fields in non-grid-based setups. [15], for example, uses a particle-based approach. This method is sound when the modelled quantity is dense in space as the particle interactions can serve as a proxy to model a field. However, this approach is not well-suited for our case as the data points are relatively sparse. [14] attempts to learn an approximation of PDEs using graph networks but are a bit orthogonal to our problem for they rely on a fixed mesh and get simulated values corresponding to nodes of the mesh. In particular, it does not have the

problem of extrapolating the prediction to values that are measured outside this fixed mesh.

(Conditional) Neural Processes (CNP) [3] introduces an efficient way of conditioning the prediction of a model on a set of measurements. Data points $f(x)$ are first encoded using an MLP and then averaged to construct a single latent vector. To make a prediction another MLP takes as input the query location and this latent vector. In practice, we find that summing the latent vectors into a single vector creates a bottleneck and that hinders the training of the model. This fact was already noticed in previous works [7].

Architectures incorporating the Fourier Neural Operator (FNO) recently introduced in [10] have been used to develop “black box” PDE solvers. The basic building block of the FNO is per token linear transformation combined with Fourier Transform. The inductive bias of this model is that solving PDEs in the frequency space is more natural than trying to work on the original space. Fourier Transforms are doing a kind of position-mixing operation which seems to be necessary for this kind of task. In this work, we compare our model to FNO in two different setups first by adapting our model to their large grid-spaced dataset and then by extracting a non-regular setup from their regular dataset.

Transformers [17] have been spectacularly successful in sequence modelling. Starting from Natural Language Processing, they have become the standard architecture for many tasks including computer vision [2], neural radiance fields [6], and reinforcement learning [11]. A strength of the Transformer architecture is that it offers an efficient way of conditioning a prediction on other information.

Our Transformer architecture follows closely the original Transformer architecture [17] and the set Transformers [9] variant as it uses the same encoder-decoder structure. Set Transformers leverage as well as the permutation-invariant nature of the attention mechanism to apply it on sets, but their original implementation restricts it to classification tasks. We show in this work that the encoder-decoder architecture provided by Transformers is also applicable to extrinsic predictions.

3 Extrinsic Forecasting

The goal of the different models in this work is to extrapolate from a context of measurements that are measured irregularly in an underlying space and to extrapolate from them, to make accurate forecasts at other positions in space, in particular outside the domain of the context set that the models have at their disposal.

We use the notation of [1] simplified to a single input and single output metric space, using the standard def-

inition of distance as the default metric. Let $\mathbb{X}, \mathbb{I}, \mathbb{O}$ be three bounded metric spaces, and define two functions $f : \mathbb{X} \rightarrow \mathbb{I}$, mapping from data to the input space, and $g : \mathbb{X} \rightarrow \mathbb{O}$ mapping to the output space. We want to learn a *Spatial Function Transformation* (SFT) which maps a function f to g . We only have access to f by data $(c_x, c_y) \in \mathbb{X} \times \mathbb{I}$ of measures c_y at position c_x and we know g only through a set $(t_x, t_y) \in \mathbb{X} \times \mathbb{O}$ of measurements t_y at position t_x . Note that \mathbb{I} and \mathbb{O} might be different so c_y and t_y do not necessarily belong to the same metric space. So we learn SFTs from data using multiple sets of measures corresponding to many (f, g) pairs to minimize the distance in the output metric space \mathbb{O} between predictions and references.

Models We consider only models that can generate predictions conditioned on a context set. This means that these models take as input not only one tensor but a tuple of tensors (c_x, c_y, t_x) corresponding to context and query positions to output forecast \hat{t}_y corresponding to the queried positions. We adapted the original encoder-decoder Transformer architecture so that it encodes the context in a permutation-invariant manner, and we compared it first to the model that we developed during our previous work GKA [12]. As previously mentioned GKA is only applicable if the input space \mathbb{I} is the same as the output space \mathbb{O} as it forms the prediction as a weighted average of the context values. This property is only valid for the wind nowcasting task and therefore we only compared this model to others on that task. We then compared them to other deep learning approaches [3, 1]. We add a schematic description of every model used in that comparison in the Appendix 7.

4 Experiments

All experiments are performed using PyTorch [13], and all data is available under permissive open-source licenses. To compare the different models we arrange the configuration so that each model has roughly the same number of parameters. A similar parameter count obviously does not imply a similar capacity or “size”, but given the architecture, we are comfortable broadly comparing models of equal parameter counts. We then evaluated the different models at three different scales of parameters. All models are implemented in a common framework, with the same encoder and decoder in each case. This is to ensure that the difference in performance lies in the architectural design of the different models. We use the same optimizer for each model with only a different learning rate (chosen via grid search) and kept the same other hyperparameters constant. The exact configurations can be found in Appendix 7.6 and the whole set of experiments can be reproduced with our codebase.

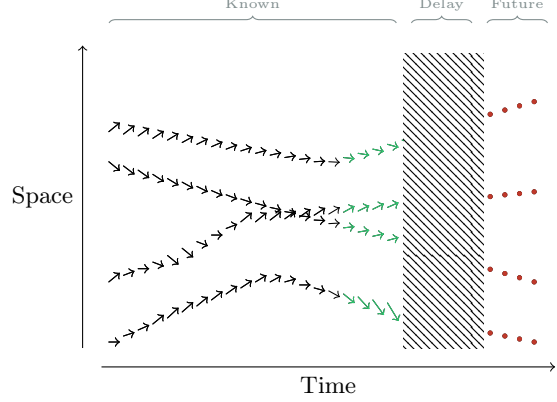


Figure 1: Schematic demonstrating the data split so that only known data can be used for prediction. This is done by slicing the dataset into pairs of time slices separated with a delay corresponding to the prediction horizon. The first element of the pair is the context and the second is the target values. Green arrows represent the context value (c_x, c_y) , and red dots represent the points where the prediction should be made (t_x) . All these points are fed to the different models to output a prediction.

Encoding scheme In [17], Transformers use a positional encoding of the linear token embeddings to encode the position of elements in the sequence. We do not need this feature because the order of the elements in the context is not important for prediction. However, we have evaluated four different methods to encode the position and value of the measures: linear embedding, positional encoding, both combined, and a feed-forward network. We report the results of this experiment in Appendix 7.7. We use a feed-forward layer because it gives better results and was used by default by GEN and NP.

4.1 High-Altitude Wind Nowcasting This section describes an important task for ATC: predicting wind at high altitudes using the live measures broadcasted by airplanes. Here, the underlying space is European airspace, $\mathbb{X} = \mathbb{R}^3$. In particular, for the z direction, most of the values are recorded at high altitudes, between 4,000 and 12,000m. At these altitudes, ground-based measurements are not available and we must rely on measurements taken by airplanes themselves. As planes do not record the wind in the z direction, the input space corresponds to wind speed in the x, y plane $\mathbb{I} = \mathbb{R}^2$, and the output space is the wind speed measured later $\mathbb{O} = \mathbb{R}^2$. In this particular setup, the models need to extrapolate in time, based on a set of the last measurements.

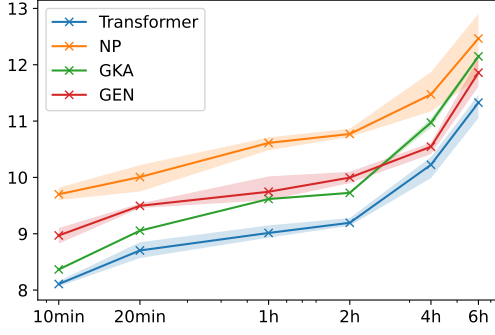


Figure 2: RMSE of the different models depending on the forecast duration (lower is better). We ran three experiments varying the pseudorandom number generator seeds for each time window and each model to measure the standard deviation. The error is not increasing drastically over the first two hours due to the persistence of the wind measures.

Airplanes measure wind speed with a sampling frequency of four seconds. We split the dataset into time slices, where each slice contains one minute of data, such that each time slice contains between 50 and 1500 data points. We tried different time intervals but noticed that having a longer time slice did not improve the quality of the forecasts. The objective for the different models is to output a prediction of the wind at different query points 30 minutes later. We evaluate the model using Root Mean Square Error (RMSE).

Smart averaging strategies such as GKA are limited by design to the range of the value contained in their context. However, these baselines are powerful as they are not prone to overfitting and in the case of time series forecasting, if the underlying variable has some persistence, the last values would in general be the best predictor of the next value. We hypothesize that over sufficiently short horizons, these methods would be similar to the performance that we get with other more complicated models but that when the window of prediction increases they will be limited by their design.

We plot the performance of the different models in the function of the time window in minutes [Fig 2]. We chose the configuration of each model such that they have around 100,000 parameters and we ran three different seeds.

We see that Transformers perform better than other models for any forecast duration. We see as well that GKA achieves quite good performance when the time horizon is low as most of the information contained in the context is still up-to-date, but when the time-horizon increases, this model suffers from its lack of flexibility and we see that over that range GEN is more

competitive.

Since, for extrinsic forecasting, target points need not lie in the convex hull of context points, the greater flexibility of Transformers makes it possible to make correct forecasts that are impossible with GKA. Figure 3a demonstrates this fact, with a plot of the target variable, the context points and the context convex hull in wind speed space.

But greater capacity means also more failure modes. As we saw in the results Table 1, Transformer is the only model to outperform GKA whereas other models, even if they are more flexible, fail to beat this baseline. On average 27% of the predictions were outside the convex hull of the context. In Figure 3c we analyze the percentage of measurements outside the convex hull produced by the different models. We can see that GKA is limited whereas the other models can compensate and predict values outside the convex hull.

For all models, we can plot the norm of the input gradients to see how changing a given value would impact the prediction [Fig. 4]. We see that Transformers seem to find a trade-off between taking into account the neighbouring nodes and the global context.

4.2 Poisson Equation Next, we demonstrate the effectiveness of Transformers on a PDE problem from [1]. Problem data is in the form of a mixed boundary condition: the temperature at the boundaries is a prescribed constant, the interior of the house is a small number of constant inhomogeneities, and all other interior points obey the Laplace equation 4.2. A deep learning model is trained to predict the scalar-valued temperature function over the two-dimensional unit cube given the input data, and ground truth data in the form of $(x, y, \text{temperature})$ tuples evaluated at arbitrary input points.

Our approach encodes the five-dimensional input data $(x, y, \text{an indicator for whether the data is at the boundary, the temperature if at the boundary and zero otherwise, the heating rate if not at the boundary and zero otherwise})$ using a simple MLP, and similarly with the query points x', y' . The source and target are then passed to a Transformer, which emits an output that is decoded by a MLP to the scalar-valued prediction.

The error metric is the mean squared error (MSE) between ground truth and model predictions, we use this loss so that it's coherent with the original work [1]. Duration is in seconds/epoch. All quantities are aggregated over ten fittings at different pseudorandom number generator seeds. We optimized the original pipeline¹

¹Available at https://github.com/FerranAlet/graph_element_networks

Table 1: Results of the High-Altitude Wind Nowcasting. Each model ran for 10 epochs on an NVIDIA GeForce GTX 1080 Ti. This low number of epochs is due to the amount of data which is considerably larger than in the other experiments. The standard deviation is computed over 10 runs. We choose the configuration of the models so that every model has a comparable number of parameters. We trained all models using Adam [8] with a fixed learning rate of 10^{-3} . To initialize GEN we used k -means over the whole training set with $k = 1000$. We indicate in bold the best models for each size and we underline the best model overall. We use an RMSE loss as in [12].

Model	Size	Train RMSE (\downarrow)	Val RMSE (\downarrow)	Duration [s] (\downarrow)
GEN [1]	5000	11.02 ± 3.19	9.84 ± 2.92	30.74 ± 7.13
	20000	9.98 ± 0.76	9.24 ± 0.35	28.84 ± 5.57
	100000	9.56 ± 0.21	9.23 ± 0.44	29.32 ± 5.35
GENFixed [1]	5000	11.41 ± 0.37	9.40 ± 0.19	29.55 ± 2.31
	20000	10.60 ± 0.65	9.74 ± 0.77	26.69 ± 5.90
	100000	10.49 ± 1.79	9.67 ± 0.79	31.06 ± 3.84
GKA [12]	5000	10.65 ± 0.07	9.14 ± 0.01	6.91 ± 1.05
	20000	10.69 ± 0.06	9.13 ± 0.01	7.26 ± 1.26
	100000	10.72 ± 0.06	9.14 ± 0.01	42.65 ± 106.18
NP [3]	5000	11.94 ± 0.78	10.19 ± 0.21	7.28 ± 1.71
	20000	10.19 ± 1.83	10.11 ± 0.20	8.33 ± 1.88
	100000	10.17 ± 1.24	10.20 ± 0.26	8.40 ± 1.88
Transformer (Ours)	5000	9.86 ± 0.21	8.75 ± 0.14	18.05 ± 3.67
	20000	9.69 ± 0.38	8.70 ± 0.06	17.90 ± 2.92
	100000	9.55 ± 0.19	<u>8.67 ± 0.07</u>	19.73 ± 1.93

so that the models replicate the results of the original work (while running 20 times faster!). This is mostly due to increasing the batch size and the vectorization of the code.

We followed a slightly different approach to train the models than in the original work. Our GEN and GENFixed reimplementation only uses one graph, that is fixed at initialization, or else optimized on the training set. The original work contains one graph per scenario, corresponding to a group of samples that have the same source and sink positions and where only the coefficient and boundary condition vary. In the original work, the authors optimized the node position on the test set as well in a meta-learning fashion, while only training the GEN parameters on the training set. We choose to use only one graph trained on the training set as for the other application we do not have access to the target value at prediction time and so we are not able to train them, and we found that approach to be more sound. We see that using that approach GEN seems to lose its advantage over its fixed counterpart. We notice as well that even GENFixed at size 5000 obtains slightly better results, and the model seems to be less robust to the scale in the number of parameters.

4.3 Darcy Flow The datasets discussed in subsection 4.1 and subsection 4.2 are inherently irregular: the measurements are expected to lie within a compact set, but nothing can be assumed about where the input data may lie within the domain. Many problems, however, are formulated and solved over a regular grid. We were interested in understanding whether Transformers, which do not clearly make use of this additional structure, can be efficiently applied to such problems.

For this, we used the Darcy Flow test problem presented in [10]. In this experiment, we wish to predict the value of the function u , given the function a (called the diffusion coefficient), where the two are related implicitly via the following PDE:

$$(4.1) \quad \begin{aligned} -\nabla \cdot (a(x)\nabla u(x)) &= 1 \text{ if } x \in (0,1)^2 \\ u(x) &= 0 \text{ if } x \in \partial(0,1)^2. \end{aligned}$$

Mathematically Equation 4.1, is called the Darcy flow equation, and it occurs across fields of mathematical modelling of the physical sciences.

Data comes in the form of 1024 distinct instances of the mapping from a to u for all $(x,y) \in (0,1)^2$ on a 421×421 grid. The motivation of this paper is to use a deep neural network to develop a PDE solver that can

Table 2: Results of the Poisson equation. Each model ran for 1000 epochs on a NVIDIA GeForce GTX 1080 Ti. We compute the standard deviation by running each experiment 10 times with different seeds. We choose the configuration of the models so that every model has a comparable number of parameters. We trained all models using Adam [8] with a fixed learning rate of 10^{-3} . GENs use a 7×7 grid. We improved the efficiency of their pipeline so that it is 20x faster. We followed a slightly different approach here in that GEN only uses one graph even in the non-fixed case we learn the position of the nodes on the training set as well. We indicate in bold the best models for each size and we underline the best model overall. We used MSE loss as in the original work [1].

Model	Size	Train MSE (\downarrow)	Val MSE (\downarrow)	Duration [s] (\downarrow)
GENFixed (Original)	5000	0.002 ± 0.0001	0.044 ± 0.0028	19.979 ± 0.3912
GEN 7×7 [1]	5000	0.081 ± 0.0093	0.090 ± 0.0042	1.407 ± 0.5539
	20000	0.135 ± 0.1679	0.144 ± 0.1594	1.880 ± 0.8518
	100000	0.289 ± 0.2561	0.285 ± 0.2436	2.428 ± 1.1163
GENFixed 7×7 [1]	5000	0.033 ± 0.0354	<u>0.036 ± 0.0322</u>	1.275 ± 0.4381
	20000	0.161 ± 0.2419	0.161 ± 0.2352	1.606 ± 0.7395
	100000	0.266 ± 0.2553	0.257 ± 0.2475	2.515 ± 1.3171
NP [3]	5000	0.134 ± 0.0032	0.135 ± 0.0031	0.166 ± 0.0337
	20000	0.124 ± 0.0433	0.130 ± 0.0395	0.222 ± 0.0848
	100000	0.092 ± 0.0070	0.109 ± 0.0019	0.333 ± 0.1207
Transformer (Ours)	5000	0.057 ± 0.0136	0.072 ± 0.0087	1.135 ± 0.4877
	20000	0.032 ± 0.0096	0.056 ± 0.0091	1.030 ± 0.3979
	100000	0.028 ± 0.0256	0.054 ± 0.0144	1.631 ± 0.6468

learn the $a \mapsto u$ relationship from examples. This can be described as a SFT where $\mathbb{I} = \mathbb{R}^+$ corresponds to the measurement of the diffusion coefficient and $\mathbb{O} = \mathbb{R}$ is the solution of the PDE. \mathbb{X} is the domain over which a and u are defined, in this case $(0, 1)^2$.

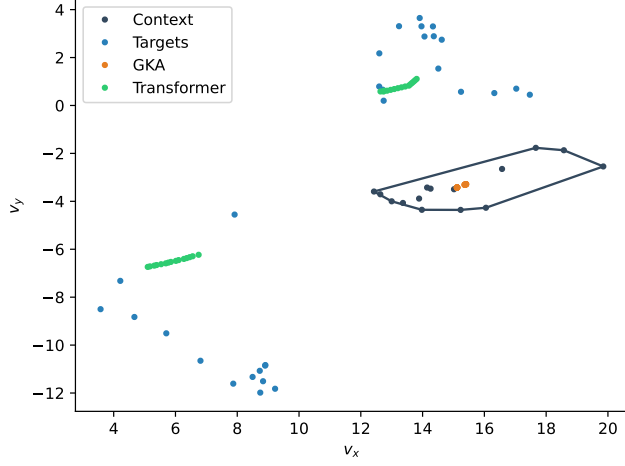
Note that interpolation (or extrapolation) of a given problem instance is not of primary interest, but rather the goal is to produce an accurate u given a previously unseen a . This is the problem we discuss in subsubsection 4.3.1. And in subsubsection 4.3.2, we adapted the setup by sampling irregularly measurements from the original grid dataset and examine whether Transformers can learn to interpolate given incomplete data on a particular PDE and how it compares to other models.

4.3.1 Regular grid comparison When the data lives on a regular grid, we can compare Transformers and the other methods discussed thus far, to the Fourier Neural Operator (FNO)-based network described in [10]. Unfortunately, attempting to process an entire $H \times W$ grid encounters the problem that the attention matrix (and thus, memory requirements) scale like $\mathcal{O}(H^2W^2)$. This is usually dealt with by using strategies to create tokens that represent multiple input units for example using patching [2] (VIT) or using a small convolutional tower. Here we use a two-layer convolu-

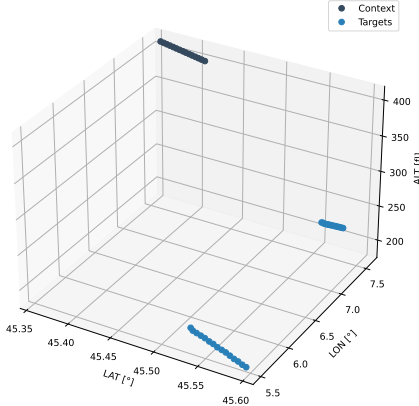
tional tower that reduces the input grid to 20×20 . We then flatten this grid structure in a sequence of 400 tokens that are concatenated with 2D positional encodings and then processed by a Transformer. We then upsample this signal with two transposed convolution layers. Each convolution in both the downsampling and upsampling modules is alternated with batch normalization and ReLU non-linearities. The results can be seen in Appendix 8, we see that in this setup the Transformer, while still beating the other reported baselines is outperformed by convolutional networks and FNO (both of which strictly require a grid structure).

An important caveat to our results: we find that FNO layers are not necessary to succeed in this problem. [10] posit that discarding lower order modes in Fourier space, is an efficient way to summarize spatial relationships in constructing intermediate features. However, we find that a small change to their experiment, replacing Fourier Transform \rightarrow truncation \rightarrow Inverse Fourier Transform logic with a simple encoder-decoder bottlenecking (strided convolution downsampling to a low dimensional space, followed by a transposed convolution upsampling), offers even better performance.²

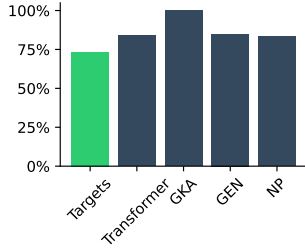
²And this is intuitive: a well-known property of the Fourier transform is that it composes with linear operations. Since there are no nonlinearities in Fourier space, networks incorporating



(a) Context, targets, and forecast in wind speed space.



(b) Context and targets in the 3D space.



(c) Percentage of the prediction values that are contained in the convex hull of the measurement in the context in percent.

Figure 3: Context and the targets in wind speed and 3D space. Both are 1min slices of data. The targets correspond to wind measurements recorded 30min after the one in the context. The forecasts of the Transformer model and the GKA model are plotted as well. GKA is restricted to predict within the convex hull of context measurements (depicted here in grey). Transformers do not suffer from this limitation.

We term this variant of the model “Bottleneck2d” in the results presented in Appendix 8. Future work will further analyze this interesting finding. And very recently we learned that [4] find similarly, replacing FNO-modules with UNet blocks. Their finding is akin to ours, though ours is even stronger (on the particular application to Darcy flow) because we do not even require skip-connections.

4.3.2 Irregular data comparison We moreover examined the Darcy Flow equation without the benefit of a regularly-spaced grid. To do this, we subsampled the regular grids uniformly at random to form a data set shaped similarly to the previous Poisson equation experiment.

As previously, we used 200 train problems for the training, each “minibatch” evaluated the loss on one such mapping from diffusion coefficients to the solution, with the loss over 32 rows of 64 grid locations each. The query consisted of 256 points. We used as a loss the relative mean square error between predictions and ground truth on test problem instances, as in the original work to measure the ability of the network to map unseen diffusion coefficients to their steady-state solution.

Table 3 a direct analogue of Table 2, but for the Poisson equation. Again, the Transformer models reach the best performance. We noticed again that Transformers seem to behave better when scaling the number of parameters. This is coherent with the results on wind nowcasting and the Poisson equation task and suggests that Transformers might be working better in more complex setups.

5 Conclusion

Transformer-based models have advanced the state of the art in numerous deep-learning domains[17, 2, 6, 11]. We have argued that Transformers are well-suited to *extrinsic forecasting*, where two types of input information are combined: (1) direct examples of the input-output relationship, and (2) auxiliary information mapping inputs to an intermediate value (associated with an output) to make two distinct types of predictions: (1) mapping from inputs to outputs, but also (2) inputs to intermediate values.

Surprisingly, “off-the-shelf” Transformers are competitive with custom architectures on several extrinsic forecasting problems that arise in modelling physical systems through time. Transformers are thus plausible models for SFTs, that is, to map between input,

$\overline{\text{FNOs}}$ are not more expressive than networks using convolution without FNOs.

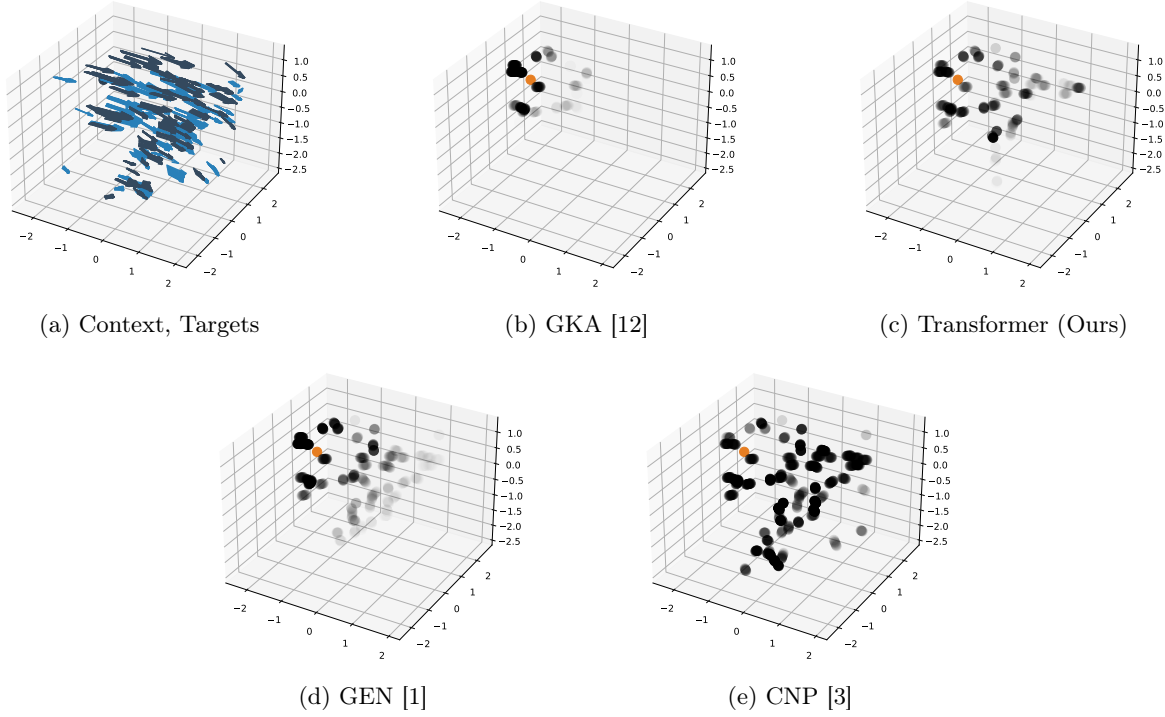


Figure 4: Displaying the importance given to points in the context to do the prediction for the different models for a given query point (orange). We used the norm of the input gradients for that purpose and highlight the context measurements that have the larger gradient with respect to the output. The opacity of the dots corresponds to the relative magnitude of the input gradients compared to other points in the context.

Table 3: Results of the Darcy Flow equation on an irregular setup. Each model ran for 500 epochs on a NVIDIA GeForce GTX 1080 Ti GPU. Standard deviations are computed over 10 experiments with different seeds. Each model has a comparable number of parameters. We trained all models using Adam with a fixed learning rate of 10^{-3} . We indicate in bold the best models for each size and we underline the best model overall. We used relative MSE as a loss as it was coherent with the original work [10].

Model	Size	Train Rel. MSE (\downarrow)	Val Rel. MSE (\downarrow)	Duration [s] (\downarrow)
GEN [1]	5000	0.022 ± 0.0006	0.034 ± 0.0007	2.155 ± 0.0324
	20000	0.022 ± 0.0013	0.034 ± 0.0015	2.874 ± 0.0357
	100000	0.022 ± 0.0024	0.033 ± 0.0015	3.761 ± 0.0412
GENFixed [1]	5000	0.025 ± 0.0033	0.034 ± 0.0022	2.170 ± 0.0271
	20000	0.022 ± 0.0028	0.032 ± 0.0011	2.889 ± 0.0360
	100000	0.058 ± 0.0751	0.064 ± 0.0650	3.903 ± 0.1021
NP [3]	5000	0.064 ± 0.0083	0.070 ± 0.0067	0.212 ± 0.0042
	20000	0.027 ± 0.0012	0.042 ± 0.0004	0.279 ± 0.0032
	100000	0.021 ± 0.0031	0.043 ± 0.0006	0.417 ± 0.0048
Transformer (Ours)	5000	0.025 ± 0.0005	0.032 ± 0.0007	1.487 ± 0.0125
	20000	0.022 ± 0.0016	0.031 ± 0.0005	1.612 ± 0.0063
	100000	0.023 ± 0.0013	<u>0.030 ± 0.0005</u>	1.934 ± 0.0246

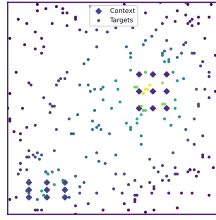


Figure 5: A sample of the Poisson Equation dataset [1]. • represents the targets, The context values are made from points in the boundaries and points on the sources and sink are represented by ♦ which corresponds to their thermal coefficient.

intermediate, and output spaces. By casting direct information as keys, and intermediate values as queries, Transformers can learn spatial structure that has previously been encoded in the model architecture, for example through convolution or graphs.

Our main application area, forecasting wind speed given sparse data, is an example of extrinsic forecasting that Transformers appear to be well-suited for. We have further benchmarked Transformers against existing deep-learning models, showing that Transformers were able to reach the best accuracy while using no external structure. Our results add to a growing literature documenting the empirical success of Transformers in tackling problems across domains. Transformers can condition predictions on different types of information, such as topography, or other weather forecasting source. Likely, this will enable further improvements to the quality of our model predictions. These perspectives might be part of future work.

Acknowledgement Arnaud Pannatier was supported by the Swiss Innovation Agency Innosuisse under grant number 32432.1 IP-ICT – “MALAT: Machine Learning for Air Traffic.” Kyle Matoba was supported by the Swiss National Science Foundation under grant number FNS-188758 “CORTI”.

References

- [1] F. ALET, A. K. JEEWAJEE, M. B. VILLALONGA, A. RODRIGUEZ, T. LOZANO-PEREZ, AND L. KAEHLING, *Graph element networks: adaptive, structured computation and memory*, in International Conference on Machine Learning, PMLR, 2019, pp. 212–222.
- [2] A. DOSOVITSKIY, L. BEYER, A. KOLESNIKOV, D. WEISSENBORN, X. ZHAI, T. UNTERTHINER, M. DEGHANI, M. MINDERER, G. HEIGOLD, S. GELLY, J. USZKOREIT, AND N. HOULSBY, *An im-*

age is worth 16x16 words: Transformers for image recognition at scale, ICLR, (2021).

- [3] M. GARNELO, D. ROSENBAUM, C. MADDISON, T. RAMALHO, D. SAXTON, M. SHANAHAN, Y. W. TEH, D. REZENDE, AND S. M. A. ESLAMI, *Conditional neural processes*, in Proceedings of the 35th International Conference on Machine Learning, J. Dy and A. Krause, eds., vol. 80 of Proceedings of Machine Learning Research, PMLR, 10–15 Jul 2018, pp. 1704–1713.
- [4] J. K. GUPTA AND J. BRANDSTETTER, *Towards multi-spatiotemporal-scale generalized pde modeling*, 2022.
- [5] T. J. HUGHES, *The finite element method: linear static and dynamic finite element analysis*, Courier Corporation, 2012.
- [6] M. M. JOHARI, Y. LEPOITTEVIN, AND F. FLEURET, *Geonerf: Generalizing nerf with geometry priors*, Proceedings of the IEEE international conference on Computer Vision and Pattern Recognition (CVPR), (2022).
- [7] H. KIM, A. MNIH, J. SCHWARZ, M. GARNELO, A. ESLAMI, D. ROSENBAUM, O. VINYALS, AND Y. W. TEH, *Attentive neural processes*, in International Conference on Learning Representations, 2019.
- [8] D. P. KINGMA AND J. BA, *Adam: A method for stochastic optimization*, 2014.
- [9] J. LEE, Y. LEE, J. KIM, A. R. KOSIOREK, S. CHOI, AND Y. W. TEH, *Set transformer*, in International Conference on Machine Learning, 2019.
- [10] Z. LI, N. B. KOVACHKI, K. AZIZZADENESHELI, B. LIU, K. BHATTACHARYA, A. STUART, AND A. ANANDKUMAR, *Fourier neural operator for parametric partial differential equations*, in International Conference on Learning Representations, 2021.
- [11] V. MICHELI, E. ALONSO, AND F. FLEURET, *Transformers are sample efficient world models*, arXiv preprint arXiv:2209.00588, (2022).
- [12] A. PANNATIER, R. PICATOSTE, AND F. FLEURET, *Efficient wind speed nowcasting with gpu-accelerated nearest neighbors algorithm*, 2021.
- [13] A. PASZKE, S. GROSS, S. CHINTALA, G. CHANAN, E. YANG, Z. DEVITO, Z. LIN, A. DESMAISON, L. ANTIGA, AND A. LERER, *Automatic differentiation in pytorch*, in NIPS 2017 Workshop Autodiff Program, 2017.
- [14] T. PFAFF, M. FORTUNATO, A. SANCHEZ-GONZALEZ, AND P. BATTAGLIA, *Learning mesh-based simulation with graph networks*, in International Conference on Learning Representations, 2020.
- [15] A. SANCHEZ-GONZALEZ, J. GODWIN, T. PFAFF, R. YING, J. LESKOVEC, AND P. BATTAGLIA, *Learning to simulate complex physics with graph networks*, in International Conference on Machine Learning, PMLR, 2020, pp. 8459–8468.
- [16] M. TANCIK, P. P. SRINIVASAN, B. MILDENHALL, S. FRIDOVICH-KEIL, N. RAGHAVAN, U. SINGHAL, R. RAMAMOORTHY, J. T. BARRON, AND R. NG, *Fourier features let networks learn high frequency functions in low dimensional domains*, NeurIPS, (2020).

- [17] A. VASWANI, N. SHAZEER, N. PARMAR, J. USZKOREIT, L. JONES, A. N. GOMEZ, Ł. KAISER, AND I. POLOSUKHIN, *Attention is all you need*, Advances in neural information processing systems, 30 (2017).

6 Appendix

7 Model description

We lay out here a schematic description of each model. We introduce the following notation for function composition: $g(f(x)) = f \triangleright g$, so that it respects the left to right convention followed by most deep learning model representation.

Recall that (c_x, c_y, t_x) are context and query positions, and \hat{t}_y is the output forecast.

7.1 Multi-Layer Perceptron A Multi-layer perceptron (MLP) block is

$$(7.2) \quad x \triangleright \text{lin} \triangleright \text{ReLU} \triangleright \text{lin} \triangleright y.$$

where lin denotes a linear mapping.

7.2 Transformers Schematically, transformers can be described as:

$$(7.3) \quad \begin{array}{l} (c_x, c_y) \triangleright \text{enc} \triangleright \underbrace{\left[\begin{array}{c} \text{sa} \\ x \end{array} \right] \triangleright \text{n} \triangleright \left[\begin{array}{c} \text{ff} \\ x \end{array} \right] \triangleright \text{n} \triangleright \nabla}_{\times N} \\ t_x \triangleright \text{enc} \triangleright \underbrace{\left[\begin{array}{c} \text{sa} \\ x \end{array} \right] \triangleright \text{n} \triangleright \left[\begin{array}{c} \text{ca} \\ x \end{array} \right] \triangleright \text{n} \triangleright \left[\begin{array}{c} \text{ff} \\ x \end{array} \right] \triangleright \text{n} \triangleright \hat{t}_y}_{\times N} \end{array}$$

where enc (dec) is a feed-forward encoder (decoder), ff is a feed-forward layer, sa and ca denotes respectively a standard self-attention and cross-attention layer, n is a layer-normalization layer. We use $[\]$ to denote residual connections.

7.3 (Conditional) Neural Processes CNP can be described as:

$$(7.4) \quad \begin{array}{l} (c_x, c_y) \triangleright \text{enc} \triangleright \text{mean} \triangleright \nabla \\ t_x \triangleright \text{enc} \triangleright \text{cat} \triangleright \text{dec} \triangleright \hat{t}_y \end{array}$$

where mean averages its inputs and cat denotes concatenation.

7.4 Graph Element Networks A GEN can be described as:

$$(7.5) \quad (c_x, c_y) \triangleright \text{enc} \triangleright c_x \mapsto \mathcal{G}_x \triangleright \underbrace{\text{mess. pass.}}_{\times T} \triangleright \mathcal{G}_x \mapsto t_x \triangleright \text{dec} \triangleright \hat{t}_y$$

where mess. pass. is a single iteration of “message passing” – averaging values with their neighbors (for more details, see [1]) and $c_x \mapsto \mathcal{G}_x$ corresponds to an interpolation between the input measures to the node position and $\mathcal{G}_x \mapsto t_x$ denotes interpolation from the nodes position to the query positions.

7.5 Fourier Neural Operator FNO can be described as:

$$(7.6) \quad x \triangleright \text{enc} \triangleright \underbrace{\left[\text{FFT} \triangleright \text{filt} \triangleright \text{lin} \triangleright \text{IFFT} \right]}_{\times T} \triangleright \sigma \triangleright \text{dec} \triangleright y$$

where filt drops lower-order modes and σ is a nonlinear activation function.

Note that FNO does not work as a context-based prediction but in that form transforms the initial condition in value at the same grid points.

7.6 Configurations The configuration of the different models are described in table 4 and 5.

7.7 Encoder As traditional transformers are constructed with discrete tokens and use positional encoding to convey the position in the sequence, we have to adapt that in our case where we want to deal with a set of measures in a permutation invariant way, while encoding continuous values. We benchmarked several approaches: the first, lin, uses only a linear layer to map the input size to a larger latent size. The second, mlp, uses a MLP to do the same. Finally, we tried to use positional encoding (pe) for these continuous values. We report the results in table 6. Following [16], we use grid search to select the normalization parameter σ , which is $1/10000$ in the original work [17], and we report the figure in table 7. Although we found that a small increase in performance can be achieved using a linear layer and a positional encoding, but we made all experiments using a MLP encoder to be consistent with other models.

8 Darcy Flow: Regular setup

We describe the results of the Darcy Flow equation in table 8. We found that using Fourier Transform was not necessary to reach the best accuracy. A model using a similar number of layers and parameters but that is replacing the specificity of the Fourier Transformer with standard convolution can reach the same performance. [4] seems to report similar findings for the Navier-Stokes equation.

Table 4: Configuration for the different models in the wind nowcasting task

Model	Size	Hidden Dim	Nb. Layers	Message Passing Steps	Nb. Heads
GEN	5000	16	1	10	
	20000	32	1	10	
	100000	64	2	10	
GEN Fixed	5000	16	1	10	
	20000	32	1	10	
	100000	64	2	10	
NP	5000	32	1		
	20000	64	2		
	100000	128	2		
GKA	5000	64	2		
	20000	128	2		
	100000	256	3		
Transformer	5000	16	1		4
	20000	32	1		4
	100000	64	1		4

Table 5: Configuration for the different models in the Poisson equation and Darcy Flow task

Model	Size	Hidden Dim	Nb. Layers	Message Passing Steps	Nb. Heads
GEN	5000	32	1	10	
	20000	64	1	10	
	100000	128	1	10	
GENFixed	5000	32	1	10	
	20000	64	1	10	
	100000	128	1	10	
NP	5000	32	1		
	20000	64	2		
	100000	128	2		
Transformer	5000	16	1		4
	20000	32	1		4
	100000	64	1		4

Table 6: Results of the different encoding schemes for the wind nowcasting task

Model	Encoder	Train norm. RMSE (\downarrow)	Val RMSE (\downarrow)
GEN	lin	0.080 \pm 0.0045	9.048 \pm 0.1231
	mlp	0.082 \pm 0.0041	9.166 \pm 0.1787
	pe	0.069 \pm 0.1873	9.014 \pm 5.9774
	pe+lin	0.083 \pm 0.0045	9.036 \pm 0.1422
NP	lin	0.101 \pm 0.0175	9.770 \pm 0.1776
	mlp	0.066\pm 0.0191	9.772 \pm 0.1810
	pe	0.072 \pm 0.2710	9.853 \pm 7.3908
	pe+lin	0.092 \pm 0.0186	9.934 \pm 0.1718
Transformer	lin	0.084 \pm 0.0025	8.576 \pm 0.0655
	mlp	0.080 \pm 0.0037	8.602 \pm 0.1034
	pe	0.080 \pm 0.2454	8.708 \pm 6.5971
	pe+lin	0.084 \pm 0.0029	8.551\pm 0.0856

Table 7: Results of the grid search of the normalization parameter γ

model	γ	Train norm RMSE (\downarrow)	Val RMSE (\downarrow)
GEN	0.000001	0.093 \pm 0.0137	9.220 \pm 0.1559
	0.00001	0.091 \pm 0.0122	9.448 \pm 0.0578
	0.0001	0.089 \pm 0.0121	9.288 \pm 0.2916
	0.001	0.087 \pm 0.0079	9.377 \pm 0.3273
	0.01	0.081\pm 0.0113	9.179 \pm 0.0221
	0.1	0.098 \pm 0.0376	10.794 \pm 2.1570
	1	0.616 \pm 0.0374	23.097 \pm 0.3862
	10	0.380 \pm 0.2220	20.505 \pm 1.5242
	100	0.310 \pm 0.0846	20.707 \pm 0.1566
	1000	0.332 \pm 0.1037	20.653 \pm 0.8183
NP	10000	0.346 \pm 0.1111	20.924 \pm 0.8919
	0.000001	0.116 \pm 0.0303	10.249 \pm 0.2224
	0.00001	0.115 \pm 0.0295	10.504 \pm 0.1200
	0.0001	0.112 \pm 0.0305	10.413 \pm 0.2710
	0.001	0.107 \pm 0.0288	10.176 \pm 0.3129
	0.01	0.104 \pm 0.0309	10.599 \pm 0.3633
	0.1	0.106 \pm 0.0467	10.967 \pm 0.4191
	1	0.844 \pm 0.0544	27.939 \pm 0.3621
	10	0.544 \pm 0.3054	24.177 \pm 6.7592
	100	0.428 \pm 0.2364	23.367 \pm 2.3993
Transformer	1000	0.370 \pm 0.1640	22.606 \pm 1.3614
	10000	0.464 \pm 0.2445	23.928 \pm 1.1282
	0.000001	0.103 \pm 0.0228	9.536 \pm 1.1127
	0.00001	0.097 \pm 0.0174	9.533 \pm 0.6911
	0.0001	0.091 \pm 0.0156	9.248 \pm 0.3734
	0.001	0.090 \pm 0.0121	9.118 \pm 0.1128
	0.01	0.085 \pm 0.0053	8.893\pm 0.2627
	0.1	0.114 \pm 0.0454	11.010 \pm 2.6034
	1	0.789 \pm 0.2129	26.511 \pm 4.7360
	10	0.191 \pm 0.0723	13.752 \pm 2.6171
	100	0.255 \pm 0.1705	16.111 \pm 5.6574
	1000	0.319 \pm 0.0972	20.184 \pm 0.9988
	10000	0.304 \pm 0.0996	19.914 \pm 1.6624

Table 8: Results of the Darcy Flow equation on a regular grid setup corresponding to an 85×85 grid. Each model ran for 500 epochs on a NVIDIA GeForce GTX 1080 Ti. We compute the standard deviation by running each experiment 10 times with different seeds. We choose the configuration of the models so that every model has approximately 1’000’000 parameters. We put in italic reported baselines (*PCANN*, *RBM*, *GNO*, *LNO*, *MGNO*), more details about them can be found in the original work [10]. We found that even in this special setup replacing Fourier Transform with regular convolution was giving better results. FNO2d denote the main model of [10]

Model	Train MSE (\downarrow)	Val MSE (\downarrow)
<i>PCANN</i>		0.0299
<i>RBM</i>		0.0244
<i>GNO</i>		0.0346
<i>LNO</i>		0.0520
<i>MGNO</i>		0.0416
ConvTower	0.0375 ± 0.0033	0.0375 ± 0.0033
FNO2d	0.0090 ± 0.0004	0.0090 ± 0.0004
Bottleneck2d	0.0079 ± 0.0013	0.0079 ± 0.0013